F & S ___ decline and resubmit

Human embryonic stem cell–derived blastocyst-like spheroids resemble human trophectoderm during early implantation process

Chaomin Yue, Ph.D. [1,#], Andy Chun Hang Chen, Ph.D. [1,2,#], Siyu Tian, B.Med. [1], Sze Wan Fong, M.Phil. [1], Kai Chuen Lee, M.Phil. [1], Jiangwen Zhang, Ph.D. [3], Ernest Hung Yu Ng, M.D. [1,2,4], Kai Fai Lee, Ph.D. [1,2,4], William Shu Biu Yeung, Ph.D. [1,2,4], Yin Lau Lee, Ph.D. [1,2,4,*]

[1]Department of Obstetrics and Gynaecology, The University of Hong Kong, Hong Kong SAR, China.
[2]Shenzhen Key Laboratory of Fertility Regulation, The University of Hong Kong Shenzhen Hospital, Shenzhen, China.
[3]School of Biological Sciences, The University of Hong Kong, Hong Kong SAR, China.
[4]The University of Hong Kong-Shenzhen Institute of Research and Innovation (HKU-SIRI), Shenzhen, China

[#] similar in author order

Professor. EHY. Ng reports grants from Ferring, personal fees from Speaker honorarium from MSD, other from Support to attend meetings from MSD, Merck, Ferring, Abbott, outside the submitted work.

Running Title: **hESC–derived blastocyst-like spheroids**

Capsule (30 words): BAP-EB possess human trophectoderm-like gene signature and can be used as human blastocyst surrogate for the study of early implantation process, endometrial receptivity and trophoblast development.

Keywords: human embryonic stem cells, trophoblastic spheroids, embryo attachment, Hippo signalling

* Corresponding author:

Dr. Yin Lau Lee (PhD): Department of Obstetrics and Gynaecology, Li Ka Shing Faculty of Medicine, The University of Hong Kong, 21 Sassoon Road, Hong Kong SAR, China.
E-mail: cherielee@hku.hk

Abstract

Objective: To study the use of human embryonic stem cell (hESC)-derived trophoblastic spheroid (BAP-EB) as human blastocyst surrogate for studying early implantation and trophoblast development.

Design: Laboratory study.

Setting: University research laboratory.

Patients/Animals: hESCs (VAL3 and H9/WA09) and endometrial aspirates donated from infertile patients.

Interventions: BAP-EB were derived from hESC. The transcriptomes of BAP-EB were analysed by next-generation RNA sequencing. The effects of Hippo signalling pathway were studied by a YAP inhibitor. The attachment of BAP-EB onto primary endometrial epithelial cells (EEC) collected at pre-receptive and receptive phases were compared. Antibody blocking assay was used to study the molecule(s) involved in BAP-EB attachment.

Main Outcome Measures: Gene expression profiles and endometrial cell attachment rates.

Results: BAP-EB differentiation protocol for VAL3 could be used to induce trophoblast differentiation in another hESC line, H9. Transcriptomic analysis showed that the epiblast signature gene expressions were reduced, while that of the trophoblast were induced during BAP-EB differentiation. Specifically, trophectoderm (TE) signature genes were induced in BAP-EB at 48h and 72h post-induction of differentiation. Hippo signalling pathway was one of the pathways induced during BAP-EB differentiation. YAP1 inhibitor significantly reduced attachment, outgrowth and trophoblast gene expressions of BAP-EB. Besides, significantly higher number of BAP-EB derived from both VAL3 and H9 attached onto receptive EEC than pre-receptive EEC. Antibody blocking assay demonstrated that endometrial E-cadherin might be critical in early implantation.

Conclusion: The data suggested BAP-EB possess TE-like signature and supported the use of BAP-EB as blastocyst surrogate for the study of trophoblast development and endometrial receptivity.

Introduction

Development of trophectoderm (TE) and its subsequent differentiation to trophoblast are critical to implantation (1). As the supply of human embryos is limited and its use for research has ethical concerns, various models have been used to decipher these developmental events. However, species-specific differences limit the extrapolation of developmental findings from animal to human (2, 3). The commonly used primary trophoblast or choriocarcinoma cell lines derived spheroids as embryo surrogates (2) also have their limitations. First, the availability of early placental tissues and proliferation of the derived trophoblast in culture are limited. Second, the choriocarcinoma cells possess cancerous characteristics and may not resemble the early embryos. Third, these mature trophoblastic cells are at developmental stages later than that of the TE (2).

To study the early trophoblastic cells, trophoblast stem cells (TSC) are derived from mouse blastocysts (4) and very recently from human blastocysts (5). Notably, Caudal Type Homeobox 2 (CDX2) which is the mouse trophectoderm genes (6) and detected at the TE of cultured E6 human embryos (7), is weakly expressed in the human TSC (5), suggesting that human TSC might not represent the TE cells in blastocysts.

Simultaneous treatments with bone morphogenic protein 4 (BMP4) and blockage of SMAD2/3 and MEK1/2 pathways induced differentiation of human embryonic stem cells (hESC) into trophoblast (8-11). To generate embryo surrogates for early implantation study, we have established the hESC-derived trophoblastic spheroids (BAP-EB) which resembled human blastocysts in size and with a blastocoel-like cavity (12). They expressed trophectodermal/trophoblastic markers. In contrast to the choriocarcinoma spheroids that attached to all the cell types tested, BAP-EB attached specifically onto receptive endometrial epithelial cells (12).

The present study aimed at studying the transcriptome of BAP-EB during differentiation and comparing with the published transcriptomes of human preimplantation embryos. We further determined the potential use of BAP-EB as a human blastocyst surrogate for studying early implantation process and trophoblast development.

Material and Methods

Human ESC culture and trophoblast differentiation

Human ESC lines VAL3 and H9 obtained from the Spanish Stem Cell Bank (Spain) and the WiCell Research Institute (USA), respectively, were maintained as described (12). BAP was used to induce trophoblast differentiation in a three-dimensional (BAP-EB) (12) format.

Isolation of endometrial epithelial cells and primary trophoblastic cells

To obtain the endometrial aspirates for isolation of epithelial cells from receptive and non-receptive endometrium, infertile women were recruited during their IVF treatments. Endometrial biopsies were taken on Day hCG+2 (n=29) or hCG+7 (n=25) when the women did not have an embryo transfer due to failure of fertilization, failure of men in submitting a semen sample after egg collection, or failure of finding sperm in testicular biopsy in men with non-obstructive azoospermia. Endometrial epithelial cells (EEC) and primary trophoblastic cells were isolated as previously described (12). Written informed consent was obtained from

all subjects recruited and the study protocol was approved by the Institutional Review Boards of the University of Hong Kong/Hospital Authority Hong Kong West Cluster (IRB: UW 16-094).

Next Generation RNA sequencing and bioinformatics analysis

RNA was extracted from 18 samples including undifferentiated VAL3 (n=2), BAP-EB differentiated for 0h (n=4), 24h (n=2), 48h (n=4), 72h (n=4) and 96h (n=2). RNA sequencing (RNA-seq) was performed by Illumina Pair-End sequencing of 101bp using Illumina HiSeq SBS Kit v4 and HiSeq PE Cluster Kit v4 cBot on an Illumina HiSeq 1500 instrument (Illumina Inc.). The average read counts were 52-64 million reads per sample. The sequencing reads generated from each sample were aligned to the human genome (UCSC hg19) with Subread aligner (http://subread.sourceforge.net/) (13). The gene count matrix was transformed into transcript per kilobase million (TPM) or count per kilobase million (CPM). Differential expression analysis was performed with R package linear models for microarray data (http://bioinf.wehi.edu.au/limma/) (14). The differentially expressed genes were identified using thresholds of FDR < 0.05 and fold change > 2.

Additional RNA-seq data from published studies were obtained from the gene expression omnibus (GEO) (Accession number: GSE36552) and ArrayExpress (Accession number: E-MTAB-3929). Single-cell transcriptomes of 1529 individual cells isolated from 88 human preimplantation embryos collected at embryonic day 3 to day 7 (E3 to E7) (15) were included in the analysis. The gene count matrices between different studies were adjusted for non-biological experimental variations using COMBAT (https://www.bu.edu/jlab/wp-assets/ComBat/Abstract.html). T-distributed Stochastic Neighbor Embedding (t-SNE) analysis was computed and plotted with Rtsne (https://github.com/jkrijthe/Rtsne). The heatmaps were plotted with gplots using z-scores calculated for each gene across different samples. The correlation plot was plotted with ggcorrplot using Pearson correlation analysis. Gene Set Enrichment Analysis (GSEA) (software.broadinstitute.org/gsea) was performed using Pre-ranked function. The gene lists from BAP-EB RNA-seq were ranked based on t-values derived from limma. The gene sets were derived from published datasets. The enrichment statistics was set as “weighted”.

Quantitative PCR and Immunocytochemistry

Quantitative PCR (qPCR) and immunocytochemistry were performed as previously described (12) using qPCR primer-probes and antibodies (**Supplemental Table S1**).

BAP-EB attachment and outgrowth

The attachment and outgrowth of BAP-EB onto endometrial epithelial cells were performed as described (12).

Cell viability assay

The Cell proliferation kit II (XTT, Roche, Sigma) was used to determine cell viability upon Verteporfin (VP, Tocris, Bio-Techne) treatment. VAL3 and H9 were seeded at 6000 and 10000 cells per well of 96-well plates (Corning). On the day of assay, the absorbance was determined by an ELISA plate reader with a wavelength of 492 nm (Infinite F200, Tecan) according to the manufacture’s instruction.

Statistical Analysis

Data were analysed and plotted using SPSS (IBM), Prism (GraphPad) and SigmaPlot software (Jandel Scientific). Statistical analysis was performed by Chi-Square test, t-test, Rank Sum test and One-Way ANOVA as appropriate. $P<0.05$ was considered as statistically significant.

Results

BAP-EB differentiation protocol is applicable in another hESC line

Using the same differentiation protocol (12), BAP-EB derived from another hESC line, H9 also possessed a blastocoel-like cavity **(Supplemental Figure S1A)**, expressed trophoblast markers **(Supplemental Figure S1B)**, secreted placental hormone βhCG **(Supplemental Figure S1C)** and attached specifically onto receptive endometrial epithelial cells **(Supplemental Figure S1D)**.

Transcriptome of BAP-EB

Eighteen RNA samples from hESC and BAP-EB at different time points post-induction of differentiation (PID) were subjected to RNA-seq. An average expression of 21,118 (83%) out of 25,343 RefSeq genes were detected in the 18 samples sequenced (**Supplemental Table S2**). We validated the sequencing data by performing qPCR on some TE specific genes (*GATA2, GATA3, KRT18, TET2, CLDN4 and CDX2*). The expressions of these genes were concordant with the same increasing/decreasing trends as those found in the RNA-seq data (**Supplemental Figure S2**).

Unsupervised hierarchical clustering showed that the samples were branched into two major clusters corresponding to un- or less-differentiated cells (hESC, BAP-EB at 0h and 24h) and differentiating cells (BAP-EB at 48h, 72h and 96h) **(Figure 1A**). T-distributed Stochastic Neighbor Embedding (t-SNE) analysis also identified the two major clusters (**Figure 1B**). We compared the expression patterns of selected functional gene sets. Epiblast (EPI) signature genes (15) were highly expressed in hESC, and BAP-EB at 0h and 24h PID but dramatically decreased from 48h PID and thereafter. On the contrary, TE (15) and trophoblast (16) signature genes were induced from 48h PID onwards **(Figure 1C)**.

Upon BAP differentiation, 770, 1898, 2286 and 2159 genes (fold change >2 and $p<0.05$) were induced in BAP-EB-24h (**Supplemental Table S3**), BAP-EB-48h (**Supplemental Table S4**), BAP-EB-72h **(Supplemental Table S5)** and BAP-EB-96h **(Supplemental Table S6)**, respectively. Gene ontology (GO) analysis showed that the most significant GO terms enriched at 48h, 72h and 96h PID included cell-cell adhesion and desmosome (**Supplemental Table S4, S5, S6**).

Transcriptome of attachment competent BAP-EB resembles that of human Day 7 polar trophectoderm

The transcriptional profiles of BAP-EB were compared to two published transcriptomes of human preimplantation embryos (15, 17). To allow comparison from these studies using different platforms and sequencing depths, we adjusted the non-biological experimental parameters between the published and our datasets using COMBAT (18). t-SNE plot showed that the hESC, BAP-EB at 0h and 24h PID intermingled with the EPI samples, while BAP-EB at 48, 72h and 96h PID intermingled with the TE samples from Yan's (17) and Petropoulos's (15) E6 and E7 **(Figure 1D)**. Unsupervised hierarchical clustering revealed similar findings **(Figure 1E)**. In addition, Pearson correlations of differentiating cells (48, 72h and 96h PID) to

TE were higher than to EPI (Supplemental Figure S3). Collectively, these results showed BAP-EB transcriptome resembled that of TE cells.

The top 500 up- or -down regulated genes between trophectoderm (TE) and epiblast (EPI) in the published data sets (15, 17) (**Supplemental Table S7**) and the differential gene lists of BAP-EB at different time points PID were subjected to gene set enrichment analysis (GSEA) (**Figure 2**). The normalized enrichment scores (NES), in which the magnitude indicated correlations between gene sets and the expression dataset, were compared between different groups. We first compared the differentially expressed genes of BAP-EB at 48h or 72h PID relative to the untreated control (0h) with the differentially expressed gene list of TE versus EPI of late blastocysts from Yan's data set (17). GSEA revealed positive NES values with the TE up-regulated genes and negative values with the EPI up-regulated genes **(Figure 2A),** suggesting that the expression profiles of BAP-EB at 48h or 72h PID were positively correlated with that of TE. The same conclusion was reached by performing similar comparison with the differentially up-/down-regulated genes in the TE of blastocysts on day 5 (E5), day 6 (E6) and day 7 (E7) in the Petropoulos's study (15) (**Supplemental Figure S4**).

GSEA comparisons were performed between differentially up-/down- regulated genes in BAP-EB-72h relative to BAP-EB-48h against the differential gene list between E5-TE versus E5 pre-lineage cells, E7-TE versus E6-TE and E6-TE versus E5-TE. Since BAP-EB-72h had the highest NES value with E7-TE up-regulated genes, the analyses indicated that BAP-EB-72h resembled most to E7-TE among other groups (**Figure 2B**).

The top 500 differentially expressed genes between E7 EPI and polar TE (pTE) or mural TE (mTE) (15) were compared against differentially expressed gene list of BAP-EB-48h versus BAP-EB-72h. GSEA analyses showed that the highest NES value was obtained between BAP-EB-72h and E7 pTE (**Figure 2C**). When compared differentially expressed genes between pTE or mTE at E6 or E7, the highest NES was observed at E7 (**Figure 2D**). We further analysed the expression ratios of the reported 135 pTE signature genes (15) in BAP-EB-72h as compared to those in BAP-EB-48h, it was found that the expression ratios of 123 out of 135 genes (>90%) matched with that between pTE and mTE (**Figure 2E**). The top 25 differentially expressed genes between E6-TE and E7-TE, and between BAP-EB at 48h and 72h were listed (**Supplemental Table S8**).

Hippo signalling is involved during BAP-EB differentiation

The top 10 enriched KEGG pathways induced after differentiation for 24h to 96h were listed **(Figure 3A)**. Hippo signalling pathway was the common pathway enriched at all time points. Hippo signalling is also one of the enriched KEGG pathways among TE up-regulated genes when compared to EPI in human blastocyst as early as E5 **(Supplemental Table S7)**. We found induction of Hippo related genes **(Supplemental Table S9)** including *YAP1*, *CDH1*, *AMOT*, *TEAD1*, *TEAD3* but not *TEAD4* during BAP-EB differentiation (**Supplemental Figure S5A**). After treating BAP-EB-24h with Verteporfin (VP) at 1.25 nM, which did not affect cell viability **(Supplemental Figure S5B)**, YAP1 immunoreacitivity was reduced in the resulting BAP-EB-72h (**Figure 3B**). The attachment rates (**Figure 3C**) and the outgrowth area (**Figure 3D**) of the treated BAP-EB on receptive endometrial epithelial cell line Ishikawa were also reduced.

The effect of VP treatment on gene expressions of BAP-EB was followed. VP treatment significantly increased the expression of pluripotent marker, *OCT4* but decreased that of CDX2 in BAP-EB-48h when compared to the untreated control ($p<0.01$). Although VP had no effect on ELF5 and GATA3, the mRNA levels of trophoblastic markers including *CDH1* at 48h PID,

CK7, and *HLA-G* at 72h PID, and *ERVW-1* (Syncytin-1) and *CGB* at 96h PID were reduced significantly upon VP treatments **(Figure 3E**).

Integrin-mediated and cell adhesion related pathways were enriched in attachment competent BAP-EB

There were 678 genes up- and 868 genes down-regulated in the attachment competent BAP-EB-72h when compared with the attachment incompetent BAP-EB-48h (fold change >2 and P<0.05, **Supplemental Table S10**). The GO terms and KEGG pathways were shown in **Supplemental Table S10.** Some genes from the induced GO clusters and KEGG pathways in BAP-EB-72h (**Supplemental Figure S6A**) were validated by qPCR and the results confirmed significantly higher expressions of these genes in BAP-EB-72h than in BAP-EB-48h (**Supplemental Figure S6B**).

BAP-EB as human embryo surrogate for the study of early implantation

The specific attachment potential of BAP-EB derived from VAL3 or H9 on primary endometrial epithelial cells (EEC) was examined. It was found that significantly higher attachment rates were obtained in EEC isolated from patients at their receptive phases (hCG+7 day) for VAL3 (Mean ± SD: 31.5± 27.1% vs. 1.8 ± 3.1%, p<0.001) and H9 (32.9 ± 22.9% vs 1.2 ± 2.3%, p<0.001) when compared to pre-receptive phases (hCG+2 day) (**Figure 4A**). Antibody blocking assay was followed by using antibodies against two attachment related molecules, E-cadherin and integrin β3 during BAP-EB attachment. It was found that a significantly lower BAP-EB attachment rate was found in the anti-E-cadherin antibody pre-treated Ishikawa cells (26.5 ± 28.2%) when compared to its normal IgG control (67.6 ± 33.0%, p<0.05) or blank control (65.3 ± 25.5%, n=5, p<0.05, **Figure 4B**). However, no difference was found when antibody against integrin β3 was used (56.1 ± 24.2% vs blank: 63.7 ± 28.1% vs rabbit IgG: 65.3 ± 32.5%, n=4, p>0.05, **Figure 4B**). The mRNA expressions of E-cadherin (*CDH1*) were significantly lower in non-receptive endometrial cell lines AN3CA and HEC1-B when compared to receptive cell lines Ishikawa and RL95-2 (**Figure 4C**).

Discussion

BAP-EB differentiation protocol was first applied to a hESC line VAL3 producing VAL3-BAP-EB (12). In the present study, we applied the same protocol to another commonly used hESC line, H9 and produced H9-BAP-EB. The characteristics of H9-BAP-EB were similar to that of VAL3-BAP-EB in terms of morphologies, marker expressions and the specificities of attachment onto endometrial cells. The data demonstrated the applicability of the differentiation protocol to different hESC lines.

To obtain the transcriptional roadmap of the hESC-derived trophoblastic spheroids, we performed RNA sequencing of BAP-EB at different time points PID. Gene clustering analysis showed that biological replicates of each time points were clustered together, indicating the robustness of the differentiation protocol. There are two major clusters separating the non-differentiated (hESC, 0h) or differentiating (24h) BAP-EB from the more differentiated cells (48h, 72h, 96h). Selected functional gene sets analysis further demonstrated the trophoblast differentiation as demonstrated by the reduced EPI signature genes (15) but induced TE (15) and trophoblast (16) signature genes expression from 48h PID onwards. We further analysed the GO terms and KEGG pathways enriched in BAP-EB. We found that cell-cell adhesion and desmosome are among the most significant GO terms enriched from 48h to 96h, in line with failure of

disaggregation of the outer cells of Day 6 expanded blastocysts into single cells due to a strongly adhered epithelium (19). Given the blastocyst-like structure and the high expression of TE signature genes, the transcriptional profiles of BAP-EB were compared to two independent studies documenting the transcriptomes of human preimplantation embryos. The clustering analysis and GSEA suggested the TE signature of BAP-EB-48h and BAP-EB-72h. We previously found that BAP-EB-72h but not BAP-EB-48h attaches specifically onto receptive endometrial epithelial cells (12). It is thus logical to assume changes in gene expression between BAP-EB-72h and BAP-EB-48h should be related to the change in attachment competency. To determine if such gene changes occurred in human embryos, GSEA comparisons were made between differentially up-/down- regulated genes in BAP-EB-72h relative to BAP-EB-48h against the differential gene list between TE cells at different developmental stages (E5, E6, E7). Interestingly, BAP-EB-72h resembled E7-TE as evident from the highest NES value in GSEA.

We further analysed the reported 135 pTE signature genes (15) and found that BAP-EB-72h closely resembled the E7 pTE while BAP-EB-48h was E7 mTE-like. These data matched with the notion that human blastocysts adhere to endometrial epithelial cells with their polar TE (pTE), the TE cells adjacent to the ICM (7, 20). Among the top 25 differentially expressed genes between E6-TE and E7-TE, and BAP-EB at 48h and 72h, genes related to cell surface receptors (TNFRSF21, MRGPRX1, CCKBR, TREML2), placental function (GJA5, MMP2), tissue remodelling (ADAMTS20) and interactome of human embryo implantation (GAST, PGC) were induced in both E7-TE (vs E6-TE) and BAP-EB-72h (vs BAP-EB-48h). On the other hands, genes that are related to ion pumps (ATP6V1B1, SLC7A3, SLC12A3) were reduced, consistent with the collapse of the cystic structure of BAP-EB at 72h PID.

The top 10 enriched KEGG pathways induced after differentiation were highly similar among different time points. Interestingly, Hippo signalling pathway was ranked first or second among the pathways enriched for the genes induced from 24h to 72h PID. Hippo signalling pathway is critical during the first cell differentiation into TE and ICM in mice (21); nuclear localized TEAD together with its coactivator YAP induce expression of genes associated with TE specification such as *Cdx2* and *Gata3* in mouse blastocysts (22). The role of Hippo signalling in human early development is not well-documented. It has been suggested that the Hippo signalling is conserved among species (23). Consistently, Hippo signalling is also one of the enriched KEGG pathways among TE up-regulated genes when compared to EPI in human blastocyst as early as E5, supporting its role in development of human TE.

YAP, one of the targets and terminal effectors of Hippo signalling, was induced at 48h and 72h PID. We therefore used a small molecule named Verteporfin (VP) that inhibited TEAD-YAP association to study the role of Hippo signalling during BAP-EB differentiation. The VP reduced YAP1 signal might be attributed to the increased YAP1 degradation. In fact, VP increased the levels of a YAP chaperon protein (14-3-3σ), which sequestrated YAP in cytoplasm and targeted them for degradation in the proteasome (24). The reduced YAP1 signal was associated with reduced attachment and outgrowth of BAP-EB onto endometrial epithelial cells, suggesting the role of Hippo signalling during early implantation process. VP treatment also reduced the trophoblast marker expressions. The observations agreed with a recent study showing that the inhibition of YAP1 and TEAD interaction by VP or YAP1 knockdown reduced the blastulation rate, hatching rate and number of $CDX2^{+}$ cells in the bovine blastocysts (25). Data obtained in the current study suggested the important role of Hippo signaling in trophoblast development leading to implantation.

When compared with the attachment incompetent BAP-EB-48h, GO terms like extracellular matrix organization, integrin-mediated signalling pathway and cell adhesion were enriched in attachment competent BAP-EB-72h. Moreover, the embryo implantation related KEGG pathways like ECM-receptor interaction, cytokine-cytokine receptor interaction and

focal adhesion were also induced in BAP-EB-72h. ECM-receptor interaction is one of the most remarkable events during mouse implantation (26). Cytokine-cytokine receptor interactions was identified as the second largest interactome during human embryo implantation (27). Focal adhesion kinase plays an important role in growth factor- and integrin-mediated cell migration (28) and regulating cell proliferation and motility during early placental development (29). On the other hand, the enriched KEGG pathways for the suppressed genes in attachment competent BAP-EB-72h were related to pathways like Wnt signalling and tight junction. The suppression of these two pathways matched with the trophoblast differentiation and disappearance of cystic structures from 48h to 72h PID.

VAL3-BAP-EB-72h but not VAL3-BAP-EB-48h attach onto receptive endometrial Ishikawa cells and can be used as embryo surrogate in an in vitro implantation assay (12). H9-BAP-EB-72h had similar property and the observations could be reproduced using primary endometrial epithelial cells (EEC). The higher attachment rates of BAP-EB onto EEC collected at receptive phases confirmed the specific interaction between BAP-EB-72h and the receptive endometrium. To test whether BAP-EB-72h can be used for the study of early implantation process, we performed antibody blocking assay during BAP-EB attachment. Adhesion molecules like integrins and cadherins play key roles in blastocyst attachment. Intrauterine injection of E-cadherin antibody (30) and Cdh1 ablation (31) reduced implantation in mice. Integrin β3 is a biomarker of endometrial receptivity (32). In agreement with others (33, 34), the mRNA expression of E-cadherin (*CDH1*) was barely detectable in non-receptive endometrial cell lines AN3CA and HEC1-B, but highly expressed in receptive cell lines Ishikawa and RL95-2. Together with another epithelial cell junctional molecule ZO-1, E-cadherin is expressed in the uterine epithelial cells at peri-implantation period (35). Clinical correlation also links lower E-cadherin expression to repeated implantation failure and recurrent miscarriage (36). The current data indicated that E-cadherin might be critical for the initial implantation process, supporting the use of the current coculture model for studying interplay between the embryo and the endometrium.

Conclusion

We showed that BAP-EB differentiation protocol is applicable to other cell lines. Transcriptomic analysis demonstrated reduction of epiblast signature genes and induction of TE and trophoblast signature genes during BAP-EB differentiation. Specifically, TE signature genes were induced in BAP-EB at 48h and 72h PID, which were associated with possession of blastocyst-like structure and acquisition of attachment competency, respectively. We also showed that Hippo signalling was involved in BAP-EB differentiation. The facts that BAP-EB specifically attached onto receptive primary endometrial epithelial cells suggested the potential use of the model for studying early implantation processes. The decision to pursue IVF treatment is difficult due to high cost, physical and psychological burden, and low success rate of the treatment. The development of a reliable predictive tool of implantation success and a better understanding of the implantation process are important in providing optimal counselling on chances of IVF success and in alleviating frustration among infertile couples with failed IVF cycles. The current model also extends the use of BAP-EB as predictive tool for assessing endometrial receptivity. In conclusion, we propose that BAP-EB is the best available embryo surrogate for study of trophoblast development and endometrial receptivity.

Acknowledgement

This work was supported in part by a General Research Fund (grant number: 17111414), Health and Medical Research Fund (grant numbers: HMRF 04151546) from the Research Grants Council of Hong Kong and National Key Basic Research Development Program (973 Program) from The Ministry of Science and Technology of the People's Republic of China (MOST 2018YFC1004402). We declare no conflicts of interest.

Figure Legend:

Figure 1: RNA-Seq transcriptome profiling of BAP-EB at different time points (A) Unsupervised hierarchical clustering of 18 samples [hESC (n=2), BAP-EB at 0h (n=4), 24h (n=2), 48h (n=4), 72h (n=4) and 96h (n=2)]. (B) t-SNE analysis showing the gene expression pattern variation among cells at different stages of differentiation. (C) Heatmaps of selected functional genes in differentiating BAP-EB. Normalized expression was plotted on a high-to-low scale (red-black-green) of genes specific to epiblast (EPI), trophectoderm (TE) and trophoblast. (D) t-SNE plot of BAP-EB (o), human early to late-blastocyst from Yan's (□) and Petropulos's (blue/green Δ) datasets. (E) Heatmaps of BAP-EB, human early to late-blastocyst from Yan's and Petropulos's datasets.

Figure 2: Gene Set Enrichment Analysis (GSEA) of differentially expressed genes in BAP-EB-48h or BAP-EB-72h verse published human blastocysts transcriptomes. GSEA of differentially expressed genes in BAP-EB-48h or BAP-EB-72h against top 500 up (upper plots) or down (bottom plots)-regulated genes between TE and EPI in Yan's study (A) or TE of different developmental days obtained from Petropoulos's study (B). (C) GSEA of top 500 up or down-regulated genes between EPI and E7-pTE or E7-mTE with the differential gene list between BAP-EB-48h or -72h verse -0h. (D) GSEA of top 500 up or down-regulated genes between mTE and pTE in E6 or E7 with the differential gene list between BAP-EB-48h and -72h. The normalized enrichment score (NES), p-value (p) and false discovery rate (FDR) are shown under each plot. (E) the expression ratios of the reported 135 pTE signature genes [21] in BAP-EB-72h as compared to 48h (black bars), and matched in the expression ratios of pTE as compared to mTE (blue bars).

Figure 3: The effects of Verteporfin (VP) on BAP-EB differentiation. (A) The top 10 KEGG pathways induced at BAP treatment for 24h, 48h, 72h and 96h over BAP-EB-0h. (B) The expression of YAP1 in VAL3 or H9 BAP-EB-72h after treated with VP or DMSO for 24h. (C) The attachment rates of VAL3 or H9 BAP-EB-72h after VP (1.25nM) treatment from 24-48h. N=5, *$p<0.05$ when compared to DMSO control. (D) The mean outgrowth area of VP treated BAP-EB-72h on Ishikawa from Day 1 (D1) to D3. D0 represent the mean size of BAP-EB after attachment. *$p<0.05$ when compared to DMSO. (E) The relative mRNA levels of *OCT4*, *CDX2*, *ELF5*, *CDH1*, *GATA3*, *KRT7*, *CGB*, *ERVW-1*, *HLA-G* and *MMP2* in BAP-EB treated with DMSO (black bars) or 1.25nM VP (grey bars) at 48h, 72h and 96h PID. hESC (white bars) was also included. *$p<0.05$ when compared between DMSO and VP treatments at the same time points.

Figure 4: BAP-EB as blastocyst surrogate for implantation study. (A) Attachment rate of BAP-EB-72h derived from VAL3 or H9 on primary EEC isolated from endometrium at hCG+2 (+2) or hCG+7 (+7) stage. *$p<0.05$, t test. (B) The attachment rates of VAL3-BAP-EB-72h on Ishikawa cells that were pre-incubated with antibodies against E-cadherin or integrin β3 (grey bars) and their corresponding IgG (white bars). Ishikawa cells without treatment (blank, black

bars) were included as controls. (C) Relative CDH1 mRNA levels in Ishikawa, RL95, HEC-1B and AN3CA EEC cell lines. $^{a\text{-}b,\ a\text{-}c,\ b\text{-}c}$ $p<0.05$.

Supplemental Figure S1: BAP-EB derived from H9. (A) Representative diagrams of H9 BAP-EB after -0h, -24h, -48h, -72h, -96h and -120h of BAP treatment. (B) The relative mRNA levels of pluripotent marker (OCT4), trophectoderm markers (CDX2 and ELF5), trophoblast marker (KRT7), STB marker (CGB) and EVT marker (HLA-G) in hESC (ES) and during BAP-EB differentiation at 0h, 48h, 72h, 96h and 120h PID. * $p<0.05$. (C) βhCG levels in H9-BAP-EB spent media collected at 96h and 120h after BAP treatment. (D) The attachment rates of H9-BAP-EB-72h (black bar) and JEG3 spheroid (grey bar) onto receptive endometrial epithelial cell line Ishikawa (Ishi), non-receptive endometrial epithelial cell lines HEC1B (HEC) and AN3CA (AN), oviductal epithelial cell line OE-E6/E7 (OE) and non-endometrial HeLa cell line.

Supplemental Figure S2: Validation of RNA sequencing. Real time quantitative analysis of TE markers (GATA2, GATA3, KRT18, TET2, CLDN4 and CDX2) during BAP-EB differentiation. The differential expression patterns were compared to the TPM values obtained in RNA-seq data.

Supplemental Figure S3: Pearson correlation plot. Correlation plot showing the distances between transcriptomes of un-differentiated (BAP-EB-0h) and BAP-EB (-24h, 48h, 72h, 96h) with TE and EPI obtained from Yan's (Y's) and Petropoulos's (P's) studies. The correlation values between each sample were obtained from Pearson correlation analysis.

Supplemental Figure S4: GSEA analysis. GSEA of differentially expressed genes in BAP-EB-48h or 72h against top 500 up (upper plots) or down (bottom plots)-regulated genes between TE and EPI obtained from Petropoulos's study. The normalized enrichment score (NES), p-value (p) and false discovery rate (FDR) are shown under each plot.

Supplemental Figure S5: Hippo signalling pathway study. (A) The relative mRNA levels of YAP1, TEAD1, TEAD3, TEAD4, CDH1 and AMOT during BAP-EB differentiation (* $p<0.05$, Mann- Whitney U test, n=5). (B) the relative proliferation rates of VAL3 and H9 during BAP differentiation from 0h to 120h with or without 0.5 (blue), 1.25 (red) and 2.5 (green) nM VP treatments. DMSO was included as controls.

Supplemental Figure S6: KEGG pathway enrichment analysis of BAP-EB-72h (verse -48h). (A) Lists of genes in BAP-EB-72h enriched KEGG pathways ($P<0.05$). (B) Real time quantitative analysis of selected genes (bold and underlined) in the KEGG pathways during BAP-EB differentiation. Statistical analysis was performed between BAP-EB-48h verse -72h (Mann-Whitney U test, *$P<0.05$, n=4).

References

1. Cha J, Sun X, Dey SK. Mechanisms of implantation: strategies for successful pregnancy. Nat Med 2012;18:1754-67.

2. Weimar CH, Post Uiterweer ED, Teklenburg G, Heijnen CJ, Macklon NS. In-vitro model systems for the study of human embryo-endometrium interactions. Reprod Biomed Online 2013;27:461-76.

3. Niakan KK, Han J, Pedersen RA, Simon C, Pera RA. Human pre-implantation embryo development. Development (Cambridge, England) 2012;139:829-41.

4. Tanaka S, Kunath T, Hadjantonakis AK, Nagy A, Rossant J. Promotion of trophoblast stem cell proliferation by FGF4. Science (New York, NY) 1998;282:2072-5.

5. Okae H, Toh H, Sato T, Hiura H, Takahashi S, Shirane K *et al.* Derivation of Human Trophoblast Stem Cells. Cell stem cell 2018;22:50-63.e6.

6. Strumpf D, Mao CA, Yamanaka Y, Ralston A, Chawengsaksophak K, Beck F *et al.* Cdx2 is required for correct cell fate specification and differentiation of trophectoderm in the mouse blastocyst. Development (Cambridge, England) 2005;132:2093-102.

7. Deglincerti A, Croft GF, Pietila LN, Zernicka-Goetz M, Siggia ED, Brivanlou AH. Self-organization of the in vitro attached human embryo. Nature 2016;533:251-4.

8. Xu RH, Chen X, Li DS, Li R, Addicks GC, Glennon C *et al.* BMP4 initiates human embryonic stem cell differentiation to trophoblast. Nat Biotechnol 2002;20:1261-4.

9. Marchand M, Horcajadas JA, Esteban FJ, McElroy SL, Fisher SJ, Giudice LC. Transcriptomic signature of trophoblast differentiation in a human embryonic stem cell model. Biology of reproduction 2011;84:1258-71.

10. Li Y, Moretto-Zita M, Soncin F, Wakeland A, Wolfe L, Leon-Garcia S *et al.* BMP4-directed trophoblast differentiation of human embryonic stem cells is mediated through a DeltaNp63+ cytotrophoblast stem cell state. Development (Cambridge, England) 2013;140:3965-76.

11. Amita M, Adachi K, Alexenko AP, Sinha S, Schust DJ, Schulz LC *et al.* Complete and unidirectional conversion of human embryonic stem cells to trophoblast by BMP4. Proceedings of the National Academy of Sciences of the United States of America 2013;110:E1212-21.

12. Lee YL, Fong SW, Chen AC, Li T, Yue C, Lee CL *et al.* Establishment of a novel human embryonic stem cell-derived trophoblastic spheroid implantation model. Human reproduction (Oxford, England) 2015;30:2614-26.

13. Liao Y, Smyth GK, Shi W. The Subread aligner: fast, accurate and scalable read mapping by seed-and-vote. Nucleic acids research 2013;41:e108.

14. Ritchie ME, Phipson B, Wu D, Hu Y, Law CW, Shi W *et al.* limma powers differential expression analyses for RNA-sequencing and microarray studies. Nucleic acids research 2015;43:e47.

15. Petropoulos S, Edsgard D, Reinius B, Deng Q, Panula SP, Codeluppi S *et al.* Single-Cell RNA-Seq Reveals Lineage and X Chromosome Dynamics in Human Preimplantation Embryos. Cell 2016;167:285.

16. Xie W, Schultz MD, Lister R, Hou Z, Rajagopal N, Ray P *et al.* Epigenomic analysis of multilineage differentiation of human embryonic stem cells. Cell 2013;153:1134-48.

17. Yan L, Yang M, Guo H, Yang L, Wu J, Li R *et al.* Single-cell RNA-Seq profiling of human preimplantation embryos and embryonic stem cells. Nature structural & molecular biology 2013;20:1131-9.

18. Johnson WE, Li C, Rabinovic A. Adjusting batch effects in microarray expression data using empirical Bayes methods. Biostatistics 2007;8:118-27.

19. De Paepe C, Cauffman G, Verloes A, Sterckx J, Devroey P, Tournaye H *et al.* Human trophectoderm cells are not yet committed. Human reproduction (Oxford, England) 2013;28:740-9.

20. Herzog M. A contribution to our knowledge of the earliest known stages of placentation and embryonic development in man. Developmental Dynamics 1909;9:361-400.

21. Nishioka N, Yamamoto S, Kiyonari H, Sato H, Sawada A, Ota M *et al.* Tead4 is required for specification of trophectoderm in pre-implantation mouse embryos. Mechanisms of development 2008;125:270-83.

22. Nishioka N, Inoue K, Adachi K, Kiyonari H, Ota M, Ralston A *et al.* The Hippo signaling pathway components Lats and Yap pattern Tead4 activity to distinguish mouse trophectoderm from inner cell mass. Dev Cell 2009;16:398-410.

23. Yu FX, Guan KL. The Hippo pathway: regulators and regulations. Genes & development 2013;27:355-71.

24. Wang C, Zhu X, Feng W, Yu Y, Jeong K, Guo W *et al.* Verteporfin inhibits YAP function through up-regulating 14-3-3sigma sequestering YAP in the cytoplasm. Am J Cancer Res 2016;6:27-37.

25. Negron-Perez VM, Hansen PJ. Role of yes-associated protein 1, angiomotin, and mitogen-activated kinase kinase 1/2 in development of the bovine blastocyst. Biol Reprod 2018;98:170-83.

26. Chen K, Chen X, He J, Ding Y, Geng Y, Liu S *et al.* Mouse Endometrium Temporal and Spatial Expression mRNA and MicroRNA Associated With Embryo Implantation. Reprod Sci 2015;22:1399-408.

27. Altmäe S, Reimand J, Hovatta O, Zhang P, Kere J, Laisk T *et al.* Research resource: interactome of human embryo implantation: identification of gene expression pathways, regulation, and integrated regulatory networks. Molecular endocrinology 2012;26:203-17.

28. Pollheimer J, Knöfler M. Signalling pathways regulating the invasive differentiation of human trophoblasts: a review. Placenta 2005;26:S21-S30.

29. MacPhee DJ, Mostachfi H, Han R, Lye SJ, Post M, Caniggia I. Focal adhesion kinase

is a key mediator of human trophoblast development. Laboratory investigation 2001;81:1469.

30. Liu G, Zhang X, Lin H, Wang H, Li Q, Ni J *et al.* Effects of E-cadherin on mouse embryo implantation and expression of matrix metalloproteinase-2 and -9. Biochem Biophys Res Commun 2006;343:832-8.

31. Reardon SN, King ML, MacLean JA, 2nd, Mann JL, DeMayo FJ, Lydon JP *et al.* CDH1 is essential for endometrial differentiation, gland development, and adult function in the mouse uterus. Biol Reprod 2012;86:141, 1-10.

32. Lessey BA, Castelbaum AJ, Buck CA, Lei Y, Yowell CW, Sun J. Further characterization of endometrial integrins during the menstrual cycle and in pregnancy. Fertil Steril 1994;62:497-506.

33. Shirane A, Wada-Hiraike O, Tanikawa M, Seiki T, Hiraike H, Miyamoto Y *et al.* Regulation of SIRT1 determines initial step of endometrial receptivity by controlling E-cadherin expression. Biochem Biophys Res Commun 2012;424:604-10.

34. Singh M, Spoelstra NS, Jean A, Howe E, Torkko KC, Clark HR *et al.* ZEB1 expression in type I vs type II endometrial cancers: a marker of aggressive disease. Mod Pathol 2008;21:912-23.

35. Paria BC, Reese J, Das SK, Dey SK. Deciphering the cross-talk of implantation: advances and challenges. Science (New York, NY) 2002;296:2185-8.

36. Yang Y, Chen X, Saravelos SH, Liu Y, Huang J, Zhang J *et al.* HOXA-10 and E-cadherin expression in the endometrium of women with recurrent implantation failure and recurrent miscarriage. Fertil Steril 2017;107:136-43 e2.

Figure 1

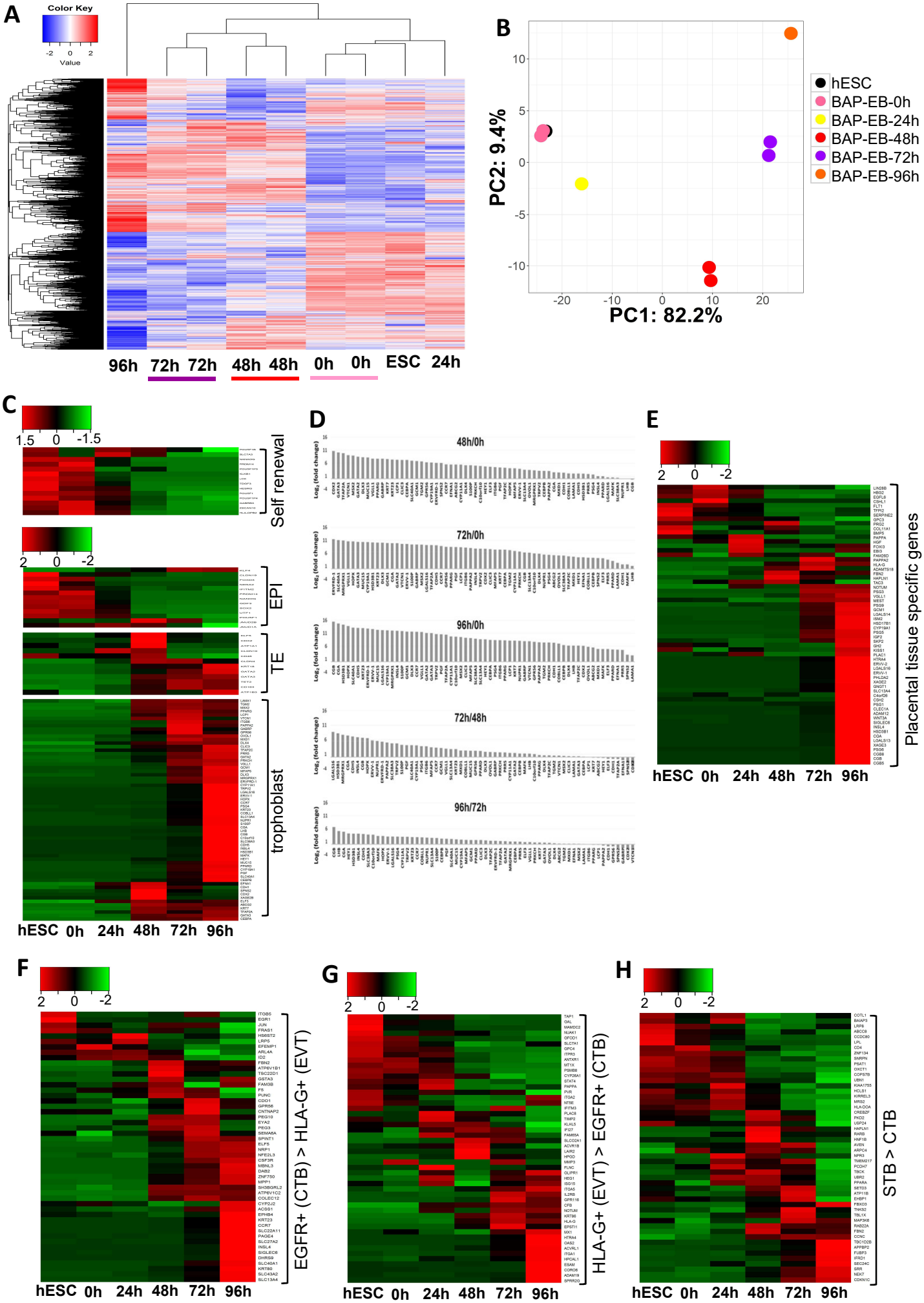
A
Color Key
-2 0 2
Value
96h 72h 72h 48h 48h 0h 0h ESC 24h
B
PC2: 9.4%
PC1: 82.2%
hESC
BAP-EB-0h
BAP-EB-24h
BAP-EB-48h
BAP-EB-72h
BAP-EB-96h
C
1.5 0 -1.5
Self renewal
2 0 -2
EPI
TE
trophoblast
hESC 0h 24h 48h 72h 96h
D
48h/0h
72h/0h
96h/0h
72h/48h
96h/72h
Log2 (fold change)
E
2 0 -2
Placental tissue specific genes
hESC 0h 24h 48h 72h 96h
F
2 0 -2
EGFR+ (CTB) > HLA-G+ (EVT)
hESC 0h 24h 48h 72h 96h
G
2 0 -2
HLA-G+ (EVT) > EGFR+ (CTB)
hESC 0h 24h 48h 72h 96h
H
2 0 -2
STB > CTB
hESC 0h 24h 48h 72h 96h

Figure 2

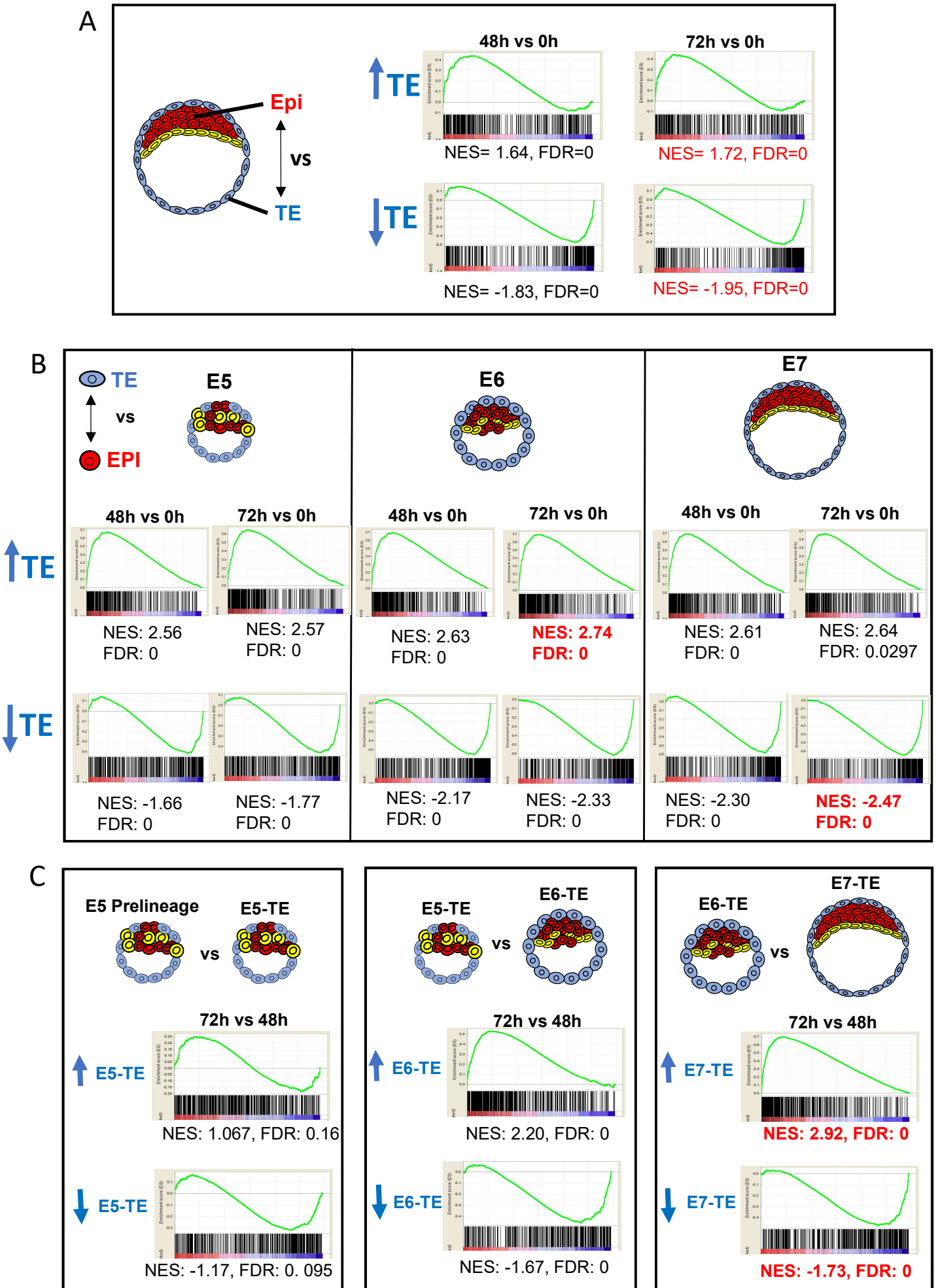
A
Epi
vs
TE
48h vs 0h
72h vs 0h
TE
NES= 1.64, FDR=0
NES= 1.72, FDR=0
TE
NES= -1.83, FDR=0
NES= -1.95, FDR=0
B
TE
vs
EPI
E5
E6
E7
48h vs 0h
72h vs 0h
48h vs 0h
72h vs 0h
48h vs 0h
72h vs 0h
TE
NES: 2.56
FDR: 0
NES: 2.57
FDR: 0
NES: 2.63
FDR: 0
NES: 2.74
FDR: 0
NES: 2.61
FDR: 0
NES: 2.64
FDR: 0.0297
TE
NES: -1.66
FDR: 0
NES: -1.77
FDR: 0
NES: -2.17
FDR: 0
NES: -2.33
FDR: 0
NES: -2.30
FDR: 0
NES: -2.47
FDR: 0
C
E5 Prelineage
vs
E5-TE
72h vs 48h
E5-TE
NES: 1.067, FDR: 0.16
E5-TE
NES: -1.17, FDR: 0. 095
E5-TE
vs
E6-TE
72h vs 48h
E6-TE
NES: 2.20, FDR: 0
E6-TE
NES: -1.67, FDR: 0
E6-TE
vs
E7-TE
72h vs 48h
E7-TE
NES: 2.92, FDR: 0
E7-TE
NES: -1.73, FDR: 0

Figure 3

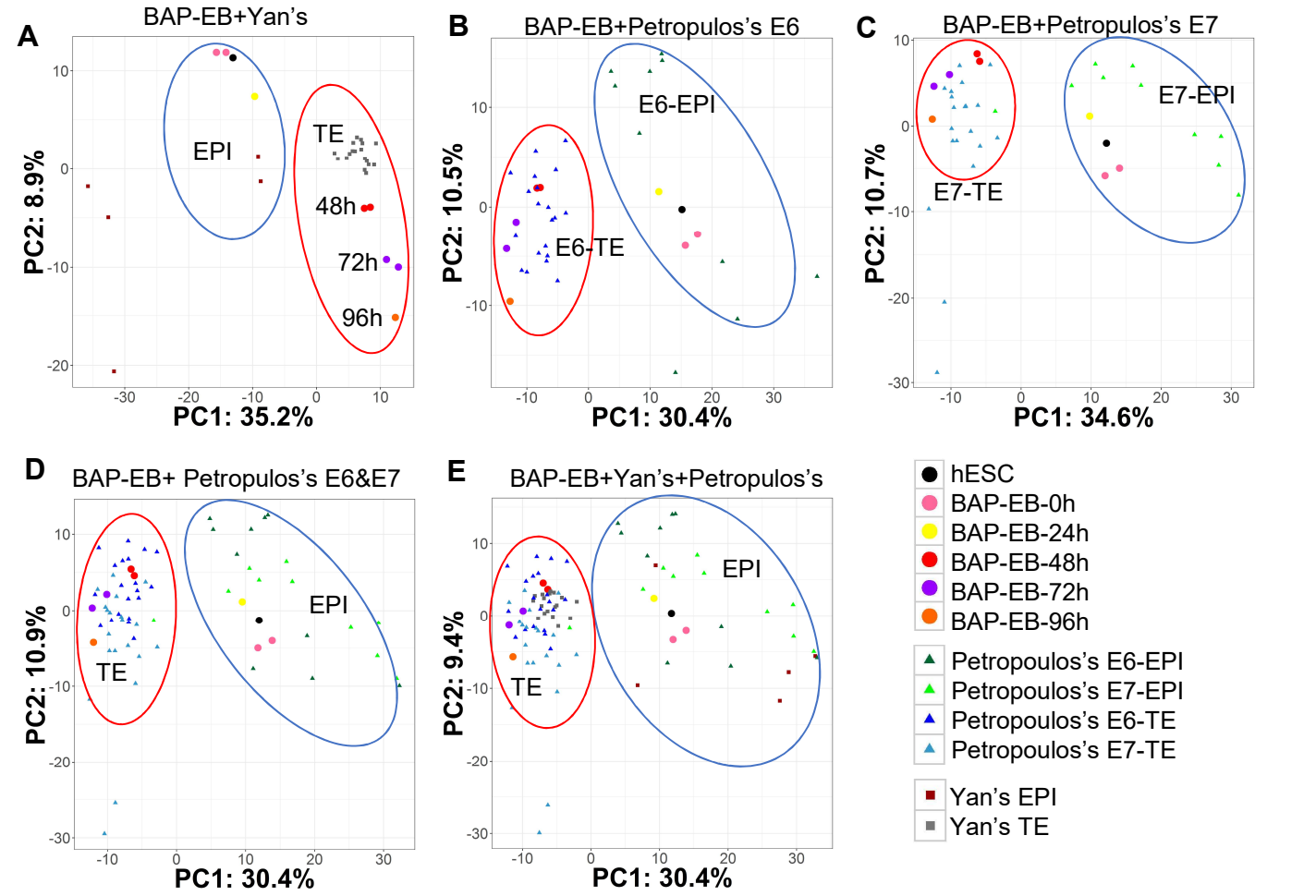
A
BAP-EB+Yan's
EPI
TE
48h
72h
96h
PC2: 8.9%
PC1: 35.2%
B
BAP-EB+Petropulos's E6
E6-EPI
E6-TE
PC2: 10.5%
PC1: 30.4%
C
BAP-EB+Petropulos's E7
E7-EPI
E7-TE
PC2: 10.7%
PC1: 34.6%
D
BAP-EB+ Petropulos's E6&E7
EPI
TE
PC2: 10.9%
PC1: 30.4%
E
BAP-EB+Yan's+Petropulos's
EPI
TE
PC2: 9.4%
PC1: 30.4%
hESC
BAP-EB-0h
BAP-EB-24h
BAP-EB-48h
BAP-EB-72h
BAP-EB-96h
Petropoulos's E6-EPI
Petropoulos's E7-EPI
Petropoulos's E6-TE
Petropoulos's E7-TE
Yan's EPI
Yan's TE

F

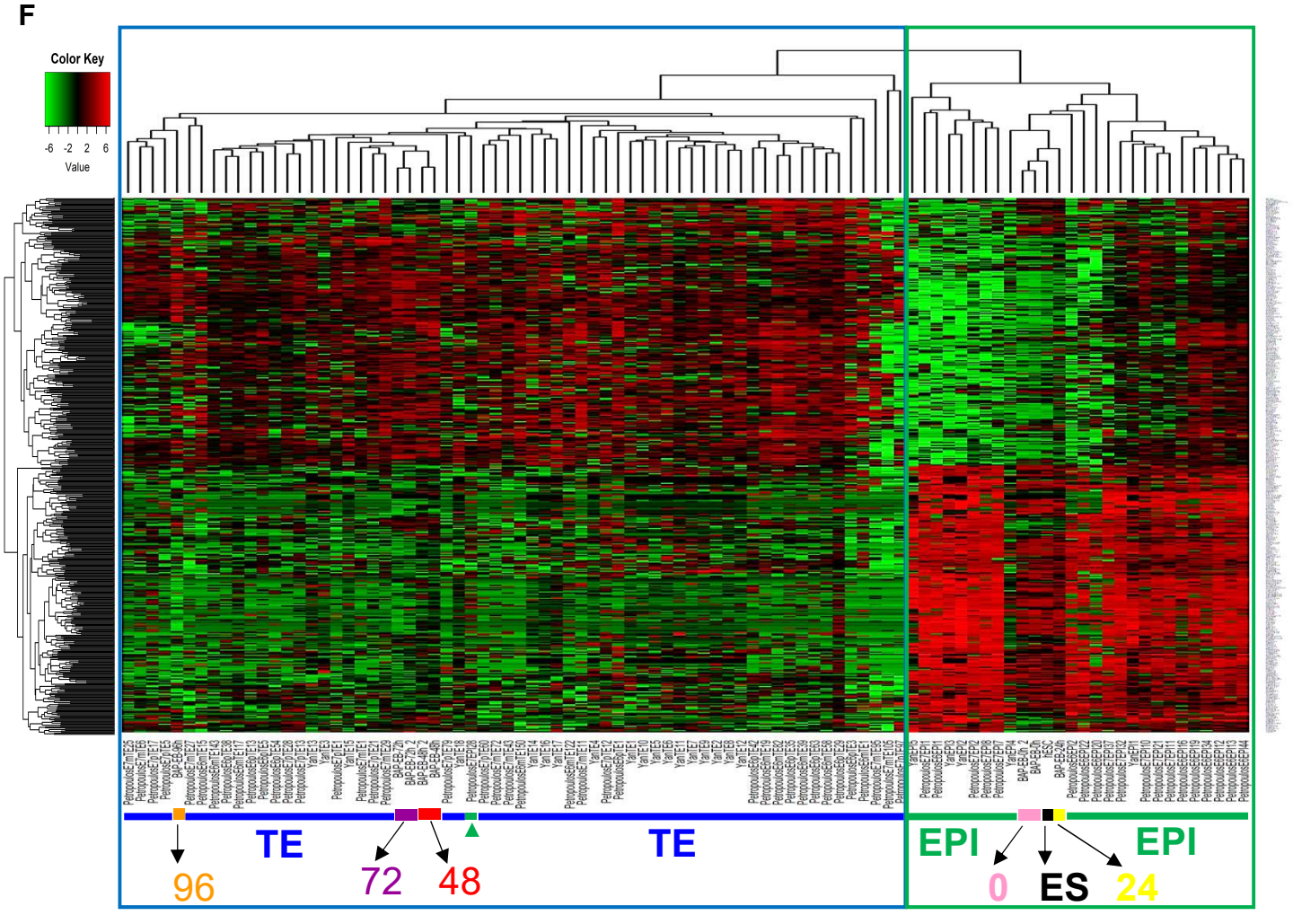
Color Key
-6 -2 2 6
Value
TE
TE
96
72
48
EPI
EPI
0
ES
24

Figure 4

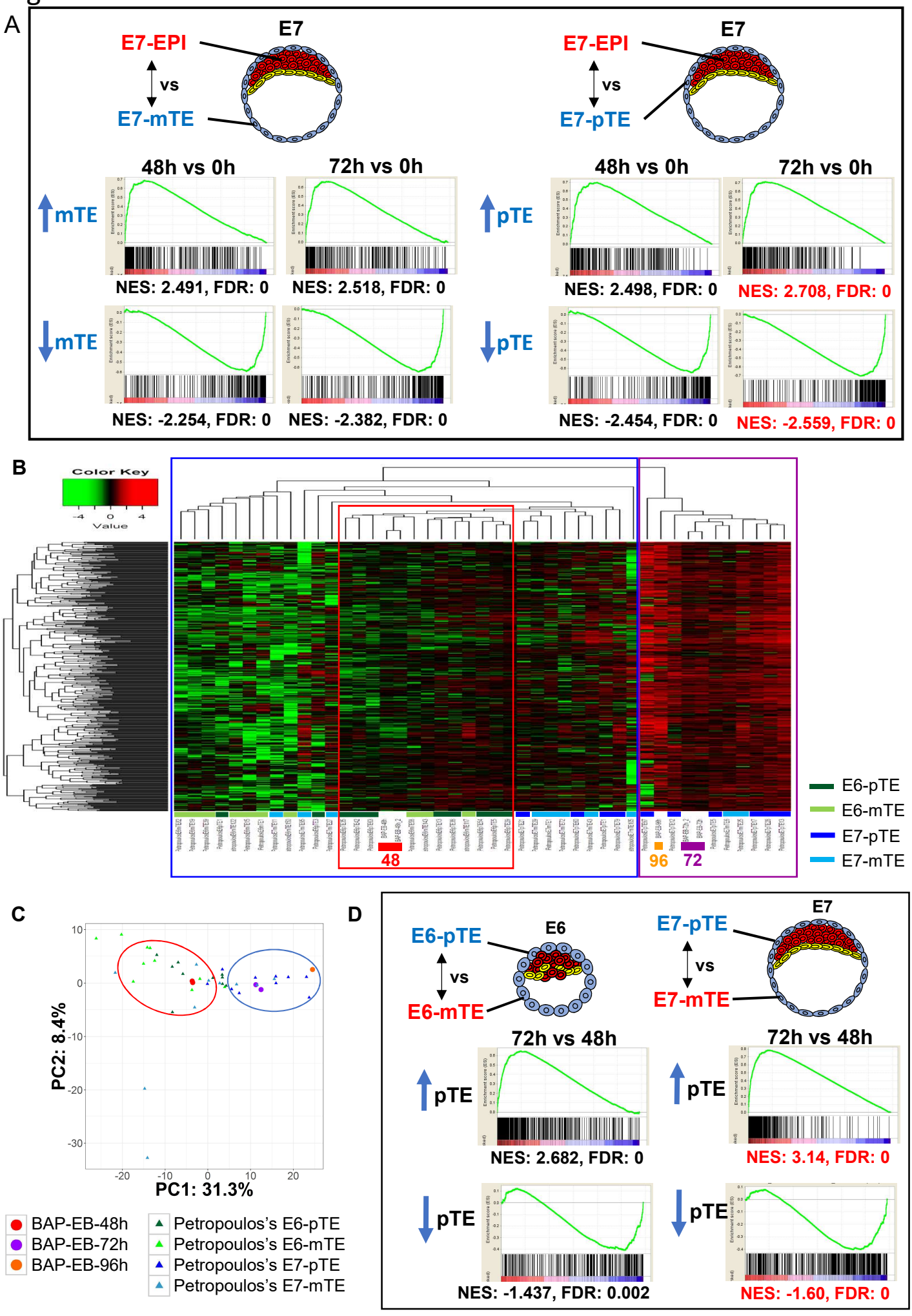
A
E7
E7-EPI
vs
E7-mTE
E7
E7-EPI
vs
E7-pTE
48h vs 0h
72h vs 0h
mTE
NES: 2.491, FDR: 0
NES: 2.518, FDR: 0
pTE
NES: 2.498, FDR: 0
NES: 2.708, FDR: 0
mTE
NES: -2.254, FDR: 0
NES: -2.382, FDR: 0
pTE
NES: -2.454, FDR: 0
NES: -2.559, FDR: 0
B
Color Key
-4
0
4
Value
48
96
72
E6-pTE
E6-mTE
E7-pTE
E7-mTE
C
PC2: 8.4%
PC1: 31.3%
BAP-EB-48h
BAP-EB-72h
BAP-EB-96h
Petropoulos's E6-pTE
Petropoulos's E6-mTE
Petropoulos's E7-pTE
Petropoulos's E7-mTE
D
E6-pTE
E6
vs
E6-mTE
E7-pTE
E7
vs
E7-mTE
72h vs 48h
pTE
NES: 2.682, FDR: 0
72h vs 48h
pTE
NES: 3.14, FDR: 0
pTE
NES: -1.437, FDR: 0.002
pTE
NES: -1.60, FDR: 0

Figure 5

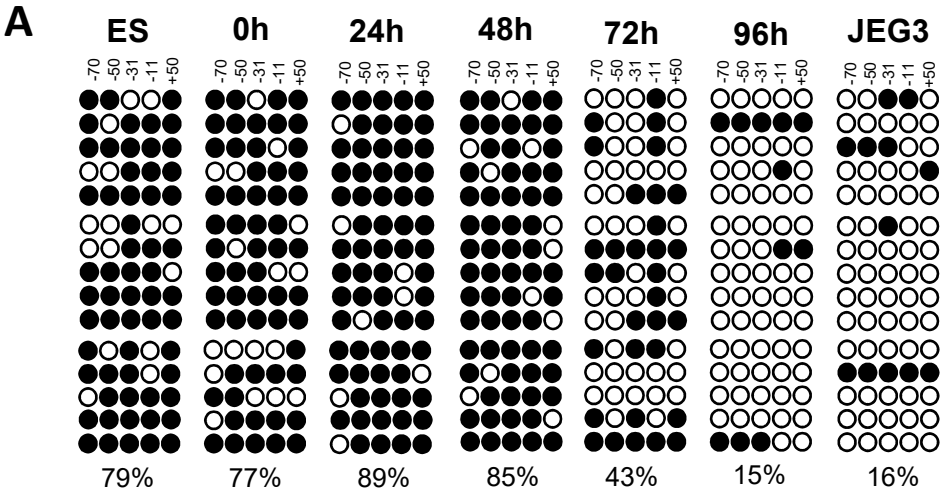

B

Position of CpG form ELF5 TSS	% of methylated cytosines				
	CpG1 (-70)	CpG2 (-50)	CpG3 (-31)	CpG4 (-11)	Average %
ES	87.97	88.03	92.07	79.29	86.84
BAP-0h	74.19	76.21	88.45	79.22	79.52
BAP-24h	88.22	86.47	87.78	80.29	85.69
BAP-48h	61.65	60.21	83.16	78.90	70.98
BAP-72h	27.42	30.57	32.54	53.21	35.94
BAP-96h	8.18	19.50	17.28	33.51	19.62
Jeg3	3.19	8.34	60.45	28.42	25.10

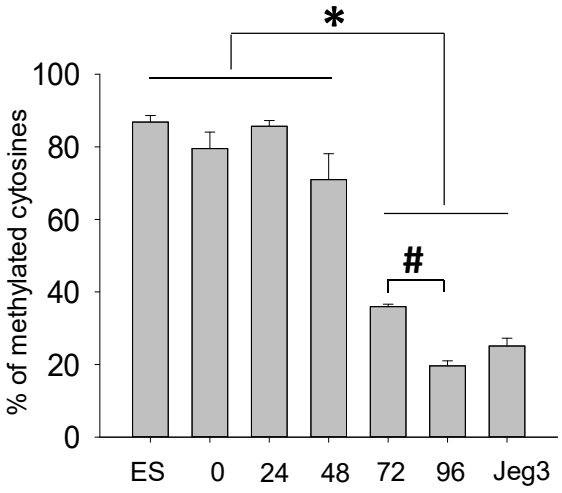

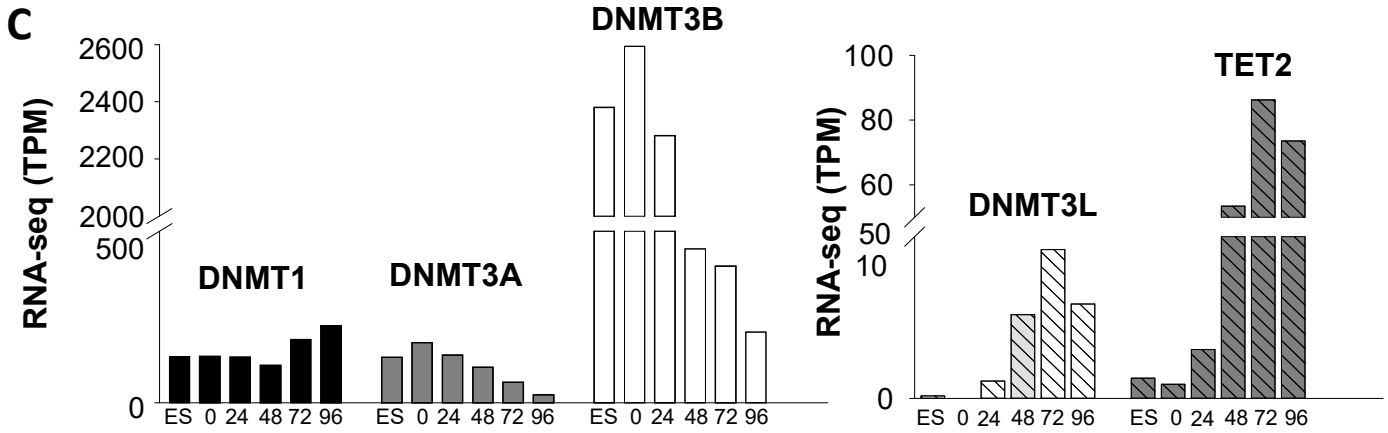

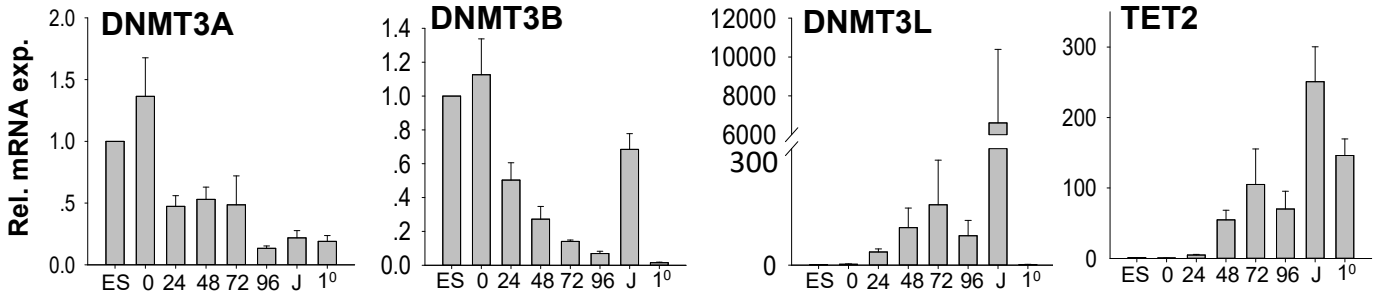

Figure 6

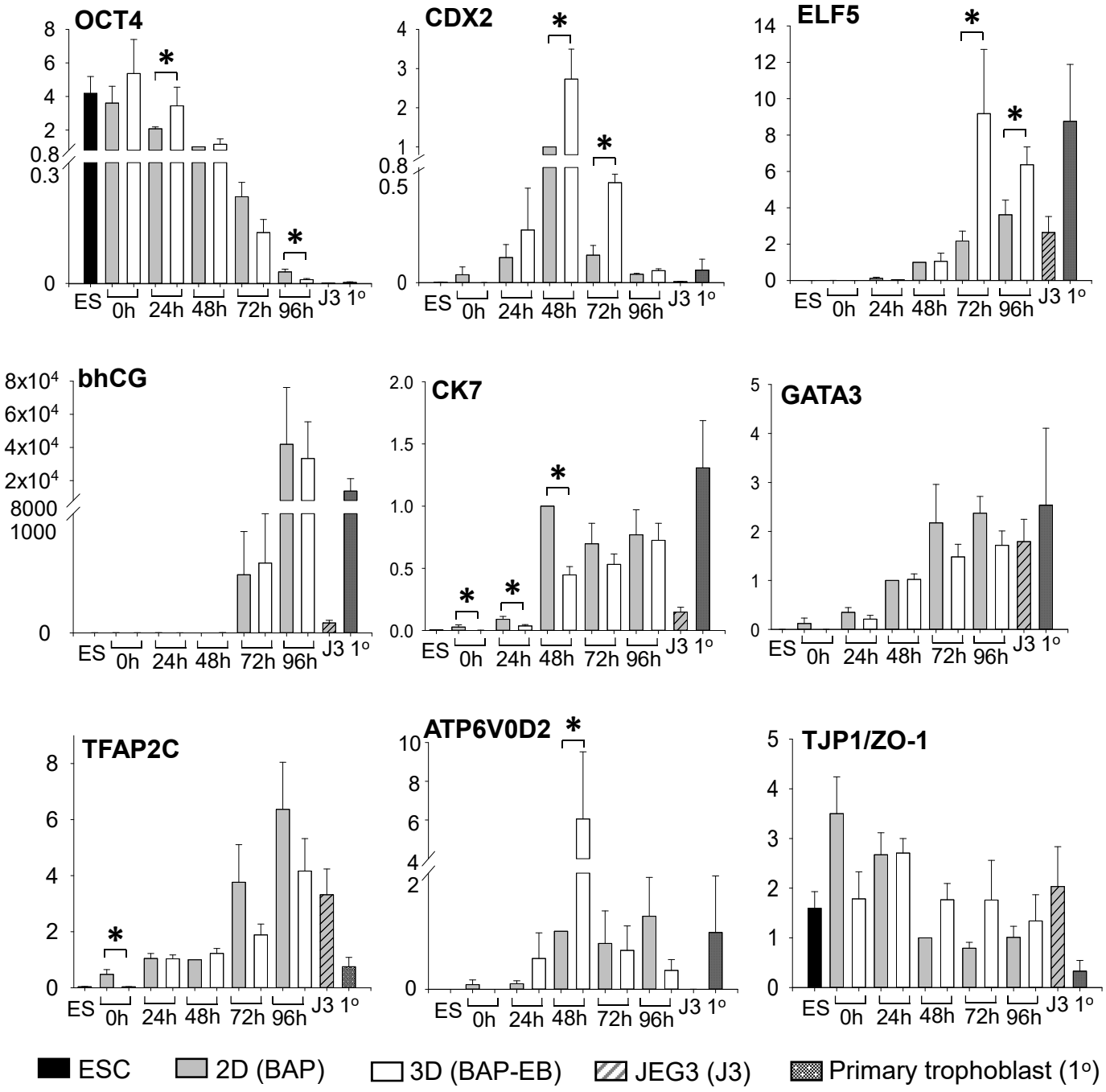
OCT4
CDX2
ELF5
bhCG
CK7
GATA3
TFAP2C
ATP6V0D2
TJP1/ZO-1
ES
0h
24h
48h
72h
96h
J3
1º
ESC
2D (BAP)
3D (BAP-EB)
JEG3 (J3)
Primary trophoblast (1º)

Figure S1

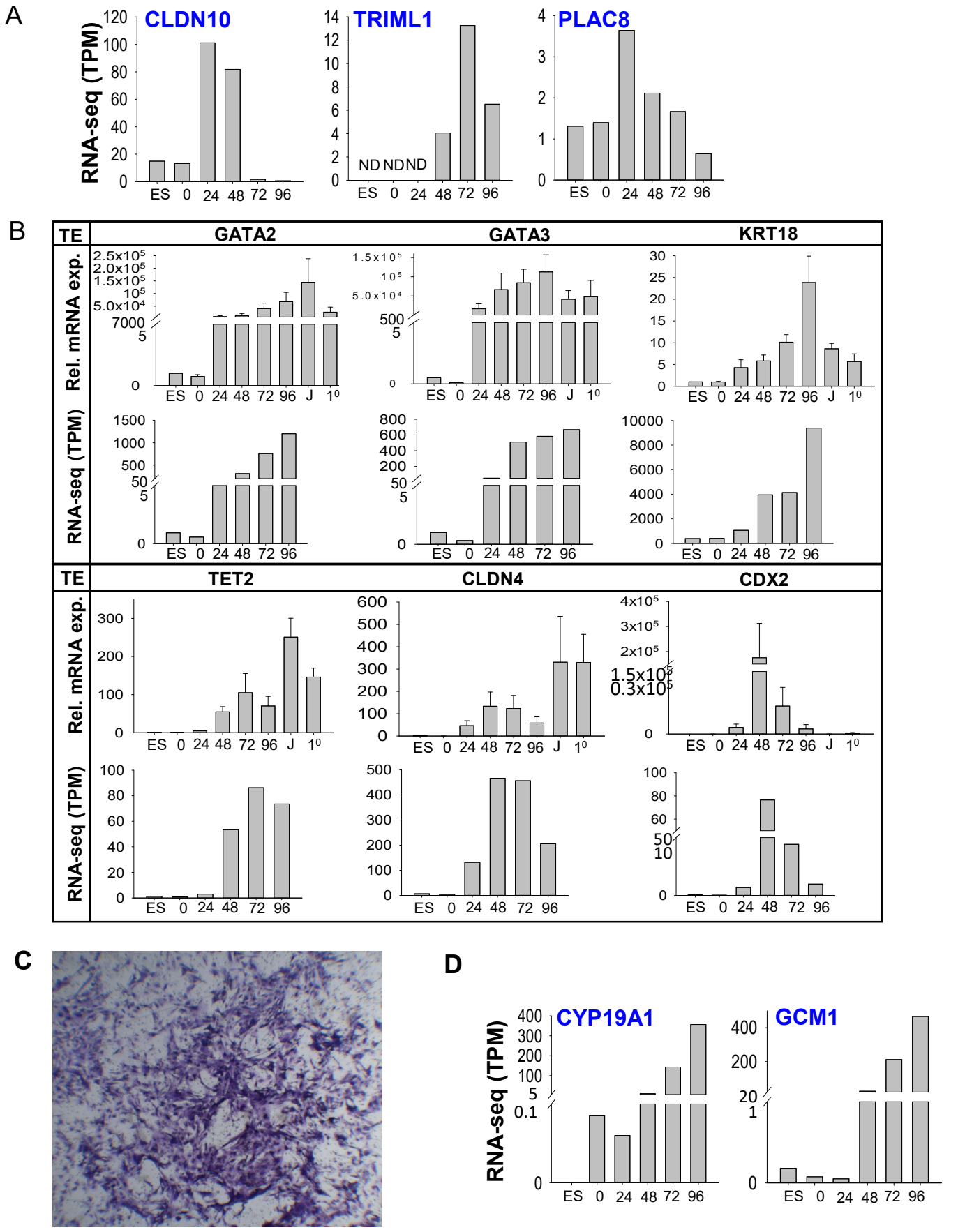

Figure S1: Transcriptome profiling of BAP-EB by RNA sequencing (related to Figure 1). (A) Plots of TPM values for selected genes (CLDN10, TRIML1 and PLAC8) showing the gene expression levels in BAP-EB at different time points. (B) Real time quantitative analysis of TE markers (GATA2, GATA3, KRT18, TET2, CLDN4 and CDX2) during BAP-EB differentiation. The differential expression patterns were compared to the TPM values obtained in RNA-seq data. (C) A representative image of the invaded cells from BAP-EB-96h in Transwell invasion assays. (D) The expression levels (TPM) of syncytiotrophoblast markers (CYP19A1 and GCM1) during BAP-EB differentiation.

Figure S2

A

KEGG pathways	Genes (72h > 48h)
Protein digestion and absorption	SLC8A3, COL4A2, COL6A6, COL21A1, COL6A5, COL3A1, COL15A1, MME, COL12A1, SLC6A19, DPP4, COL5A1, KCNE3, SLC7A7
PI3K-Akt signaling pathway	FGF18, **PDGFB**, **PGF**, OSMR, CSF1, COL3A1, ITGB4, NFKB1, TCL1B, GNG12, CCNE1, COL6A6, ITGB8, COL6A5, CSF3R, CREB3L1, CREB3L3, PIK3R1, CSF1R, EPO, ANGPT4, IL2RB, SGK1, COL4A2, ITGA1, NR4A1, BAD, EPHA2, COL5A1, ITGA9, YWHAH, IL3RA
Proteoglycans in cancer	CAV1, LUM, WNT3A, IGF2, RDX, DCN, FLNC, MMP2, TIMP3, TGFB1, CTSL, WNT7B, CBLB, FZD10, SDC1, HBEGF, WNT11, WNT7A, GPC1, PIK3R1, TWIST2
Focal adhesion	COL4A2, CAV1, **PDGFB**, **PGF**, COL3A1, ITGA1, ITGB4, ACTN2, BAD, FLNC, COL5A1, PAK6, ITGA9, COL6A6, PAK3, COL6A5, ITGB8, SHC1, PARVB, PIK3R1, PARVA
Insulin resistance	PRKCZ, PRKAG2, TRIB3, NFKB1, RPS6KA1, PYGL, SLC2A1, GFPT2, SLC27A6, CREB3L1, CREB3L3, SLC27A2, PIK3R1
HTLV-I infection	CRTC3, IL2RB, NRP1, **PDGFB**, HLA-DRB1, WNT3A, CREM, ADCY5, **TGFBR2**, **TGFB3**, NFKB1, CALR, HLA-G, TGFB1, WNT7B, FZD10, ATF3, XBP1, SLC2A1, WNT11, WNT7A, FOSL1, PIK3R1
ECM-receptor interaction	CD47, ITGA9, COL4A2, SDC1, COL6A6, ITGB8, COL6A5, COL3A1, ITGB4, ITGA1, COL5A1
Ras signaling pathway	FGF18, PLD1, **PDGFB**, **PGF**, CSF1, GRIN2A, NFKB1, BAD, GNG12, EPHA2, RASAL2, PAK6, PAK3, SHC1, KSR1, PIK3R1, RASA2, CALM1, ANGPT4, CSF1R
PPAR signaling pathway	APOA2, PPARD, ACSL1, OLR1, SLC27A6, ACSL4, FABP7, SLC27A2, ANGPTL4
Cytokine-cytokine receptor interaction	TNFRSF21, IL2RB, **PDGFB**, OSMR, CSF1, **TGFBR2**, **TGFB3**, TGFB1, **LEP**, **TNFRSF1B**, CCR7, RELT, IL1RAP, CXCR6, CSF3R, IL13RA1, IL3RA, IFNGR1, EPO, CSF1R
Steroid hormone biosynthesis	STS, HSD3B1, CYP3A7, CYP11A1, CYP11B1, HSD17B1, HSD11B2, CYP19A1

B

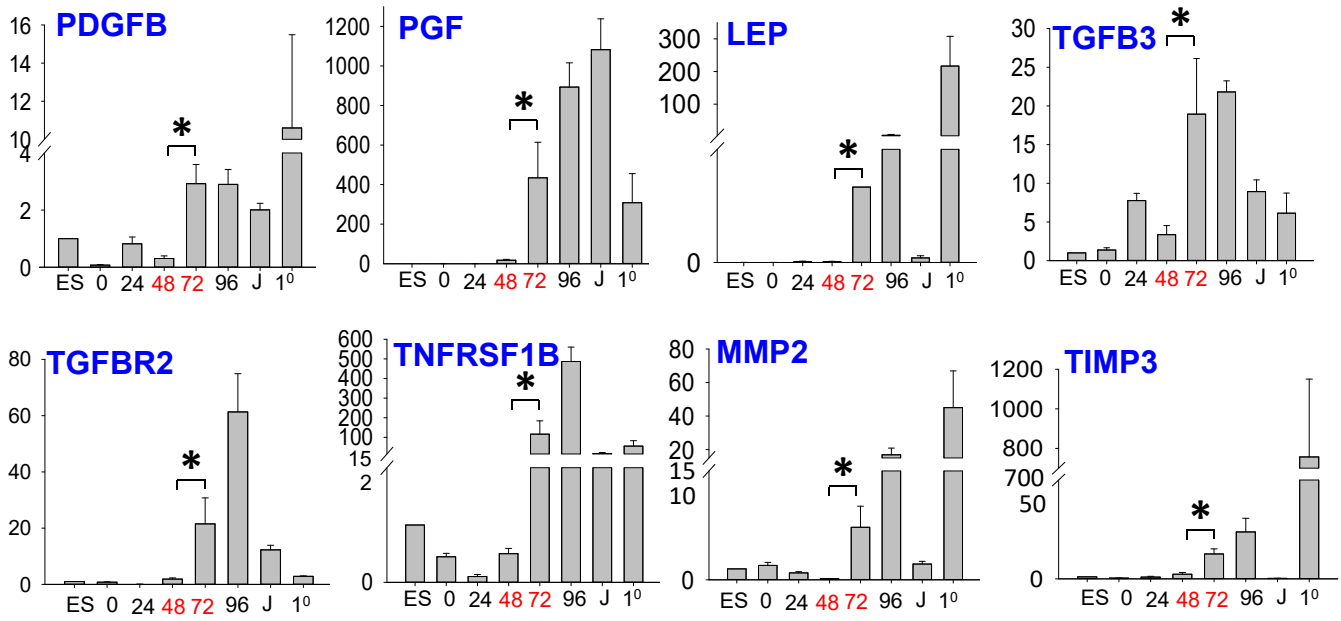

Figure S2: KEGG pathway enrichment analysis of BAP-EB-72h (verse -48h) (related to Table 1). (A) Lists of genes in BAP-EB-72h enriched KEGG pathways. (B) Real time quantitative analysis of selected genes in the KEGG pathways during BAP-EB differentiation. Statistical analysis was performed between BAP-EB-48h verse -72h (Mann-Whitney U test, *P<0.05, n=4).

Figure S3

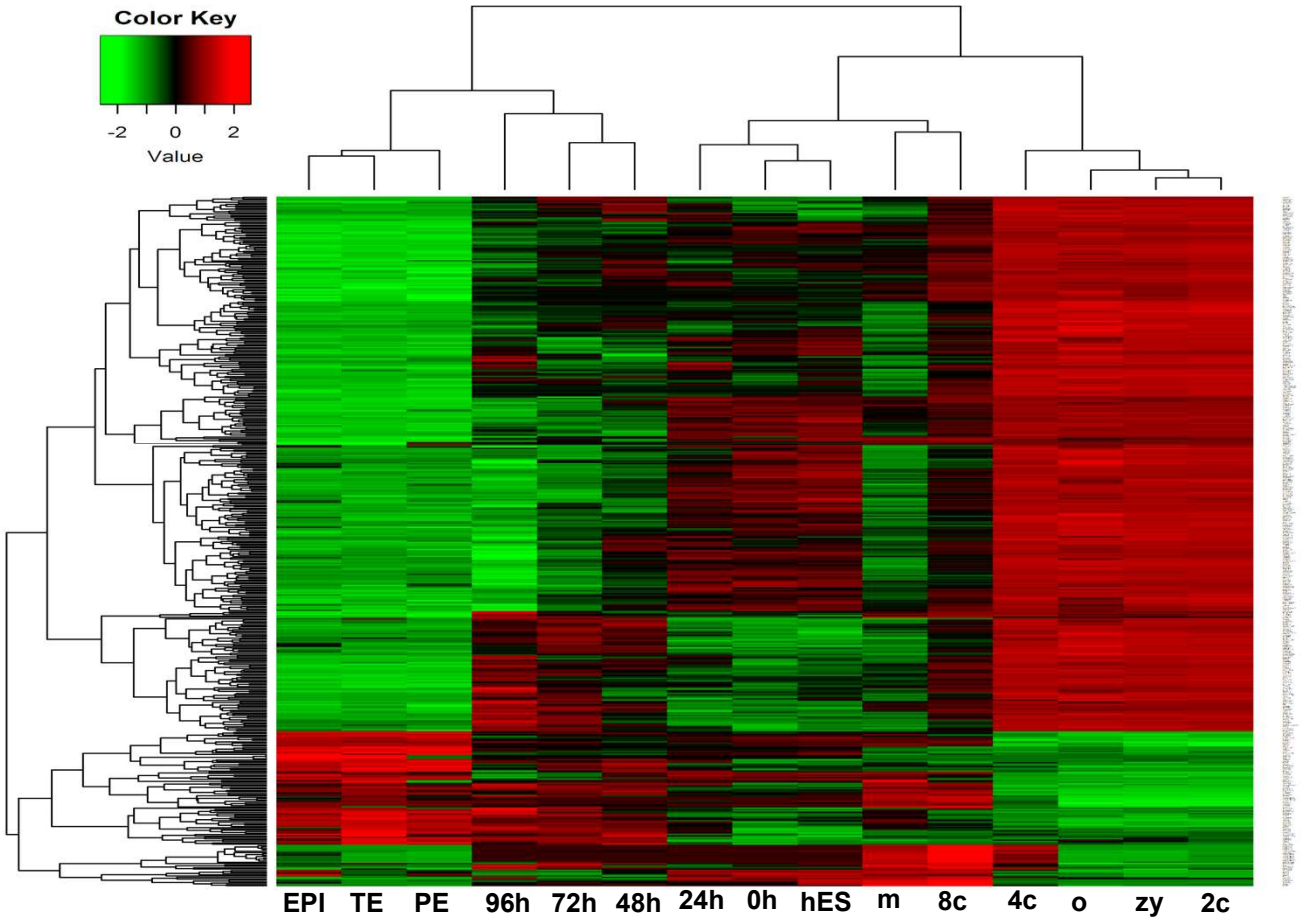

Figure S3: Unsupervised hierarchical clustering of RNA sequencing data of differentiating BAP-EB at different time points (hESC, 0h, 24h, 48h, 72h and 96h) and human preimplantation embryos (o: oocytes; zy: zygotes; 2c: 2-cell; 4c: 4-cell; 8c: 8-cell; m: morula; EPI: epiblast; PE: primitive endoderm; TE: trophoectoderm). Related to Figure 2.

Figure S4

Top 20 genes (E7-TE > E6-TE)

Gene Symbol	Gene name
GJA5	gap junction protein, alpha 5, 40kDa (connexin 40)
LGALS16	Galectin 16
GAST	gastrin
MRGPRX1	MAS-related GPR, member X1
LY6G6C	lymphocyte antigen 6 complex, locus G6C
DUSP13	dual specificity phosphatase 13
HSD3B1	hydroxy-delta-5-steroid dehydrogenase, 3 beta- and steroid delta-isomerase 1
CGB8	chorionic gonadotropin, beta polypeptide 8
TREML2	triggering receptor expressed on myeloid cells-like 2
PRR9	proline rich 9
CLEC1A	C-type lectin domain family 1, member A
ADAMTS20	ADAM metallopeptidase with thrombospondin type 1 motif, 20
LYPD5	LY6/PLAUR domain containing 5
PTPRE	protein tyrosine phosphatase, receptor type, E
CPM	carboxypeptidase M
PGC	progastricsin (pepsinogen C)
CAV1	caveolin 1, caveolae protein, 22kDa
C10orf54	chromosome 10 open reading frame 54
NUPR1	Nuclear Protein 1, Transcriptional Regulator

Top 20 genes (E7-TE < E6-TE)

Gene Symbol	Gene name
CDX2	caudal type homeobox transcription factor 2
SLC12A3	solute carrier family 12 (sodium/chloride transporters), member 3
CLDN10	claudin 10
ATP6V0D2	ATPase, H+ transporting, lysosomal 38kDa, V0 subunit d2
SCGB3A2	secretoglobin, family 3A, member 2
ALDH1A1	aldehyde dehydrogenase 1 family, member A1
TMOD1	tropomodulin 1
SATB2	SATB family member 2
FXYD4	FXYD domain containing ion transport regulator 4
GABBR2	gamma-aminobutyric acid (GABA) B receptor, 2
GLRX	glutaredoxin (thioltransferase)
ESRRB	estrogen-related receptor beta
CD53	CD53 molecule
PDPN	podoplanin
ABCC4	ATP-binding cassette, sub-family C (CFTR/MRP), member 4
ALPP	alkaline phosphatase, placental (Regan isozyme)
SLC7A3	solute carrier family 7 (cationic amino acid transporter, y+ system), member 3
NMU	neuromedin U
NRIP3	nuclear receptor interacting protein 3
RNF125	ring finger protein 125

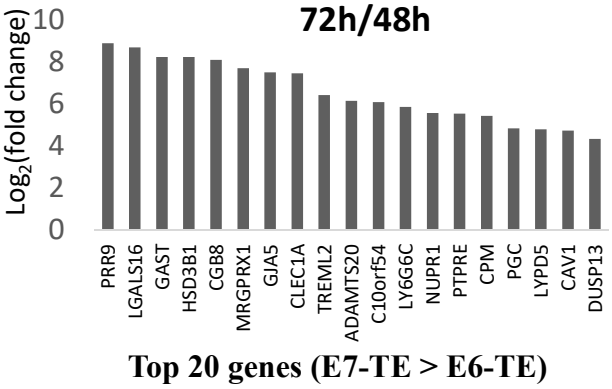

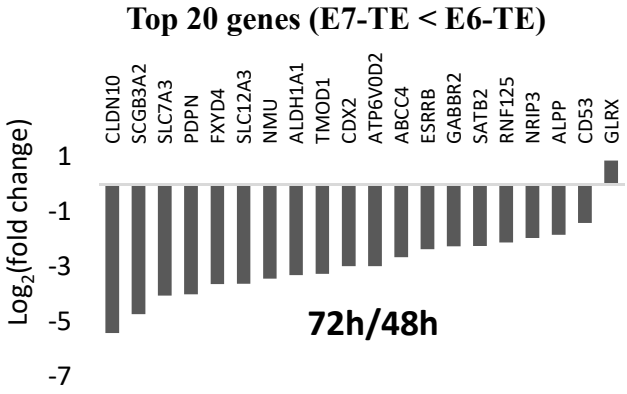

Figure S4: Common genes enriched or suppressed in attachment competent BAP-EB-72h and human E7-TE prior to implantation (Related to Figure 4). (A) Top 20 differentially expressed genes between E7-TE verse E6-TE that were also differentially expressed between BAP-EB at 72h verse 48h. (B) Folds enriched (left) and suppressed (right) of the 20 differentially expressed genes (E7-TE/E6-TE) in BAP-EB at 72h verse 48h (72h/48h).

Figure S5

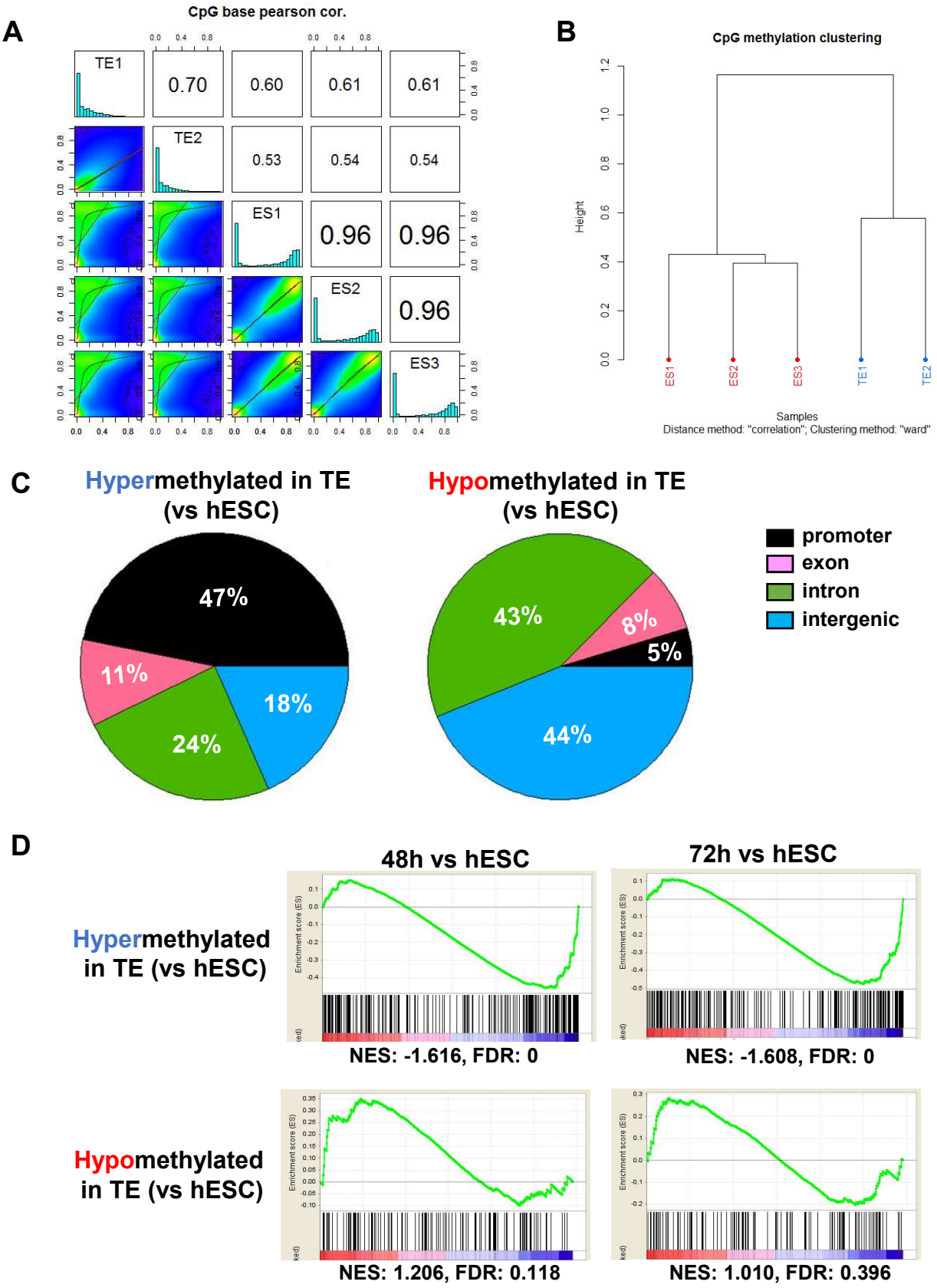

Figure S5: The relationship of the whole genome methylation status in human TE cells and the gene expression pattern in BAP-EB at 48h and 72h (related to Figure 5). (A) Pearson correlation matrix for the biological replicates of human TE and human ESC samples acquired from Smith et al., 2014 (B) Clustering of human TE and ESC global DNA methylation profiles. (C) The distribution of differentially methylated CpG sites across the mapped genes that overlapped with promoter, exon, intron or intergenic regions. (D) GSEA for determining whether top 500 differentially methylated genes between human TE and ESC samples were correlated with gene expression changes in BAP-EB. The pre-ranked gene lists were obtained according to changes in gene expression levels between BAP-EB (48h or 72h) and undifferentiated VAL3.

Figure S6

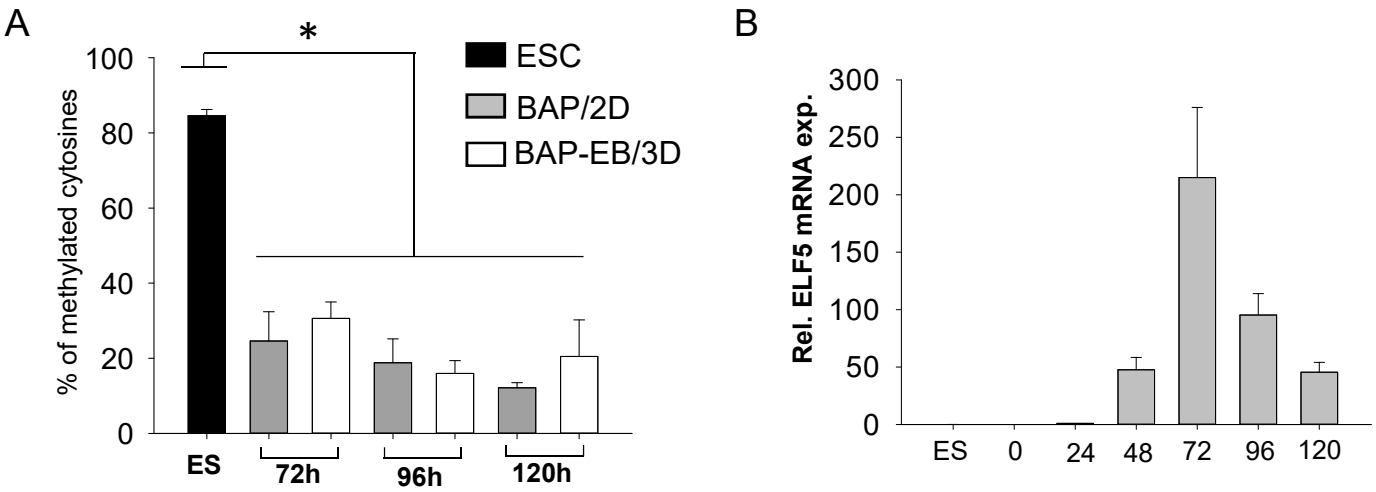

Figure S6: Correlations of DNA methylation status and gene expression of ELF5 between trophoblastic cell differentiated from two dimensional (BAP/2D) and embryoid body model (BAP-EB/3D) (related to Figure 6). (A) Pyrosequencing results of the average percentage of DNA methylated ELF5 promoter region in hESC (black bar), BAP/2D (grey bars) and BAP-EB/3D (white bars) at different differentiation time points (* $P<0.05$, Mann-Whitney U test, n=4). (B) The relative gene expression of ELF5 during BAP-EB differentiation.